JACS
JOURNAL OF THE AMERICAN CHEMICAL SOCIETY
Communication
pubs.acs.org/JACS

Photoinduced Electron Transfer Elicits a Change in the Static Dielectric Constant of a *de Novo* Designed Protein

Nicholas F. Polizzi,[†,⊥] Matthew J. Eibling,[∥,⊥] Jose Manuel Perez-Aguilar,[∥,▽] Jeff Rawson,[‡] Christopher J. Lanci,[∥] H. Christopher Fry,[∥,#] David N. Beratan,[†,‡,§] Jeffery G. Saven,*[,∥] and Michael J. Therien*[,‡]

[†]Department of Biochemistry, [‡]Department of Chemistry, and [§]Department of Physics, Duke University, Durham, North Carolina 27708, United States

[∥]Department of Chemistry, University of Pennsylvania, Philadelphia, Pennsylvania 19104-6323, United States

Supporting Information

ABSTRACT: We provide a direct measure of the change in effective dielectric constant (ε_S) within a protein matrix after a photoinduced electron transfer (ET) reaction. A linked donor−bridge−acceptor molecule, PZn−Ph−NDI, consisting of a (porphinato)Zn donor (PZn), a phenyl bridge (Ph), and a naphthalene diimide acceptor (NDI), is shown to be a "meter" to indicate protein dielectric environment. We calibrated PZn−Ph−NDI ET dynamics as a function of solvent dielectric, and computationally *de novo* designed a protein *SCPZnI3* to bind PZn−Ph−NDI in its interior. Mapping the protein ET dynamics onto the calibrated ET catalogue shows that *SCPZnI3* undergoes a switch in the effective dielectric constant following photoinduced ET, from $\varepsilon_S \approx 8$ to $\varepsilon_S \approx 3$.

Anisotropic protein interiors are often described by an effective, uniform static dielectric constant (ε_s) of 2−15.[1] The magnitude of ε_s influences critically biological electron-transfer (ET) reactions.[2] Through its effect on the pK_a of buried amino-acid residues, ε_s also impacts proton-coupled ET and proton-transfer processes.[1a,3] Theoretical and experimental studies of ET in proteins typically assume ε_s does not change as a result of the ET event.[4] In this report, we provide direct evidence for a change in the protein ε_s following ET that occurs within a *de novo* designed protein matrix.

To interrogate dynamical changes in the magnitude of protein ε_s upon photoinduced charge separation, we utilize a donor−bridge−acceptor (DBA) molecule,[5] with ET dynamics displaying marked sensitivity to (i) solvent ε_s; (ii) axial metal coordination; and (iii) deuteration of water (kinetic isotope effect). We calibrated these effects for the DBA molecule (5,15-diphenyl-10-(4′-[*N*-yl-(*N*′-(11-hydroxy-3,6,9-trioxoundecyl)-naphthalene-1,4,5,8-tetracarboxylate diimide)]phenyl-porphinato)zinc(II) (PZn−Ph−NDI, Figure 1) in a variety of organic solvents and computationally designed a tetra-α-helical protein *SCPZnI3* to bind PZn−Ph−NDI in its interior.

PZn−Ph−NDI exhibits signature photoinduced ET dynamics following preparation of the PZn-localized S_1 excited state, ^{1}(PZn)*−Ph−NDI (Figure 1A). In the low ε_s solvent system 99:1 1,4-dioxane/*N*-methylimidazole (NMI), ^{1}(PZn)*−Ph−NDI evolves to the charge-separated state $^{+\bullet}$PZn−Ph−NDI$^{\bullet-}$ with a charge separation (CS) time of τ_{CS} = 12 ps. Charge recombination (CR) to the ground state is comparatively slow: τ_{CR} = 102 ps. The ET dynamics are tracked by the rise and subsequent decay of sharp spectral features centered at 480 and 610 nm, characteristic of the NDI$^{\bullet-}$ radical anion.[6] Species-associated difference spectra (Figure 1B), derived from a global fitting of the multiwavelength transient absorption data to a sequential kinetic mechanism, also show clear signatures of the

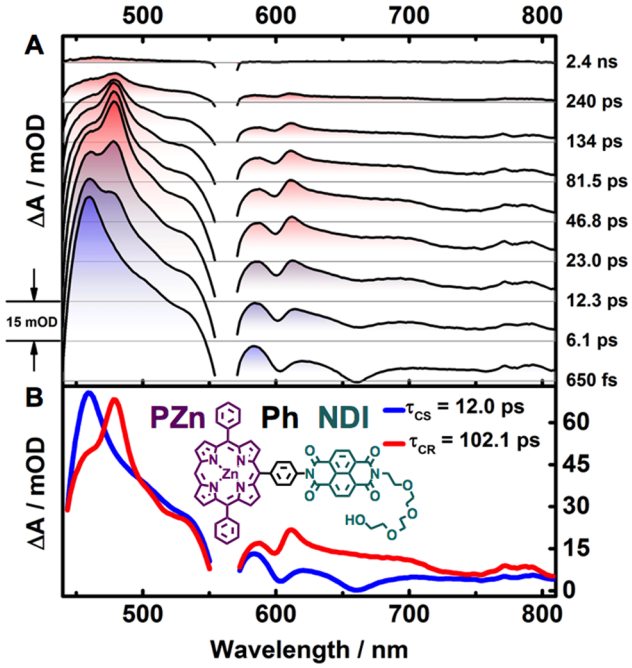

Figure 1. Pump−probe transient dynamics of PZn−Ph−NDI in 99:1 1,4-dioxane/*N*-methylimidazole. (A) Transient dynamical data at various pump−probe time delays, which are labeled on the right. Each spectrum is offset by 15 mOD for clarity. (B) Species-associated difference spectra (sans laser scatter at 560 ± 5 nm) with associated ET time constants. Experimental conditions: λ_{ex} = 560 nm, P_{ex} = 850 nJ/pulse, T = 21 °C, magic angle polarization.

Received: December 16, 2015
Published: February 3, 2016

DOI: 10.1021/jacs.5b13180
J. Am. Chem. Soc. 2016, 138, 2130−2133

$NDI^{\bullet-}$ anion (red spectrum, prominent absorbance maxima at 480, 610, and 780 nm).

Figure 2 displays the CS and CR time constants of PZn−Ph−NDI measured in organic solvents with 1% NMI. CR dynamics

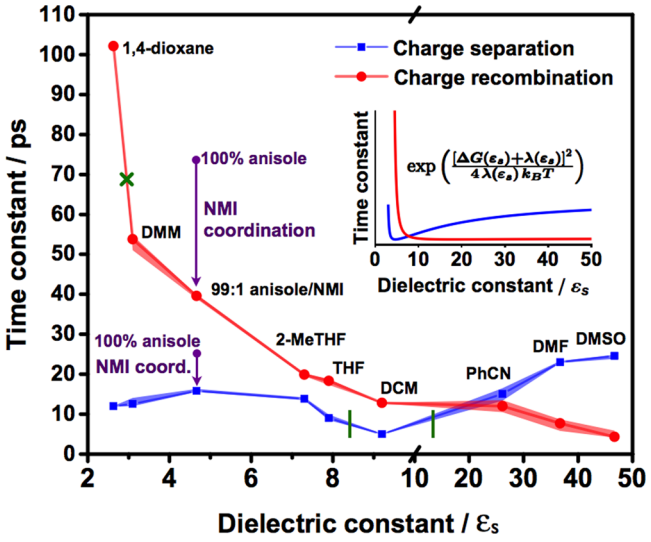

Figure 2. ET time constants τ_{CS} and τ_{CR} of PZn−Ph−NDI as a function of solvent static dielectric constant (ε_s). All solvents include 1% *N*-methylimidazole (NMI). ε_s is a volume-fraction weighted sum of component ε_s values. Shaded line widths indicate confidence intervals of the fitted time constants (bounded at 16% and 84% percentiles of the bootstrapped lifetime distributions). For the *SCPZnI3* holo-monomer, τ_{CR} is denoted with a green X. Green vertical lines mark the range of dielectric constants consistent with the measured value of τ_{CS} in the *SCPZnI3* holo-monomer. Purple arrows display an exemplary reduction of ET time constant magnitudes that occur upon NMI coordination, shown explicitly for anisole solvent. Inset: expected dielectric dependence of τ_{CS} (blue) and τ_{CR} (red) according to ET rate theory (see Supporting Information). DMM = dimethoxymethane, THF = tetrahydrofuran, 2-MeTHF = 2-methylTHF, DCM = dichloromethane, PhCN = benzonitrile, DMF = *N*,*N*-dimethylformamide, DMSO = dimethyl sulfoxide.

(red) depend strongly on ε_s, with τ_{CR} decreasing monotonically from 102 to 4 ps. CS dynamics (blue) show a τ_{CS} minimum near ε_s = 9. Indeed, the observed trends for τ_{CS} and τ_{CR} are in agreement with those expected from the Marcus activated factor of ET rate theory[2a,7] (Figure 2, inset), using parameters appropriate for PZn−Ph−NDI (Supporting Information). While the ET dynamics of PZn−Ph−NDI displayed in Figure 2 approach the low ps time regime in some solvents, all time constants are well above solvent relaxation times, such that ET is not limited by dynamic solvent effects.[8]

NMI coordination to the PZn moiety accelerates CS and CR relative to dynamics evinced in neat solvents (Figure 2, purple, and Figure S3), resulting from the more negative oxidation potential of PZn when bound to the electron donating imidazole ligand.[9] ET kinetics measured in solvents with 1% NMI provide a reference for comparison to kinetics measured within the protein environment of *SCPZnI3*, where PZn is coordinated by histidine. Accounting for axial coordination effects allows us to isolate the ε_s contribution to the ET dynamics within the *SCPZnI3* protein.

The τ_{CS} of PZn−Ph−NDI exhibits a kinetic isotope effect (KIE) in 9:1 1,4-dioxane/H(D)$_2$O mixtures (Figure 3). The KIE = $\tau_{CS}(D_2O)/\tau_{CS}(H_2O)$ decreases from 1.4 to 1.2 upon NMI coordination to PZn. Interestingly, although τ_{CR} decreases with

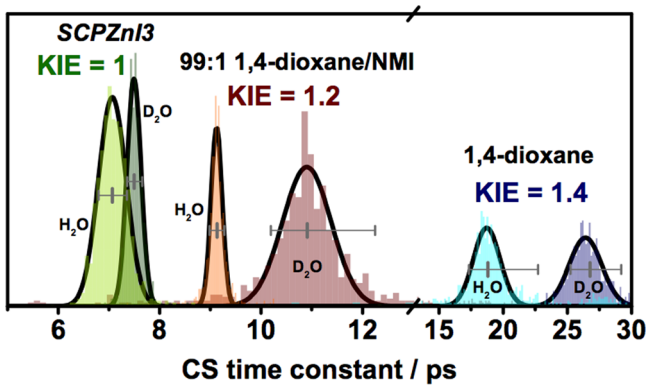

Figure 3. Distributions of CS time constant τ_{CS} displayed by PZn−Ph−NDI within various solvation environments. Distributions are derived from bootstrapping the residuals of the global fit of the pump−probe data (see Supporting Information). Measurements in 1,4-dioxane contain 10% H_2O or D_2O. Measurements with *SCPZnI3* were carried out in 50 mM NaPi/150 mM NaCl buffer with 100% H_2O or D_2O. Confidence intervals in gray display 16% and 84% percentiles of the bootstrapped lifetime distributions. The optimum time constant is shown as the middle, vertical line. Black lines overlaying the bootstrap histograms are Gaussian fits to the distributions.

increasing water content, consistent with the dielectric dependence in Figure 2, τ_{CR} does not display a KIE (Table S1, Figures S4−S7). These observations suggest that CS is more tightly coupled than CR to water H-bond interactions with the imide carbonyls.[10] The τ_{CS} KIE is an experimental probe of PZn−Ph−NDI water solvation within ground-state *SCPZnI3*.

To explore ET dynamics in a protein environment, the tetra-α-helical protein *SCPZnI3* was computationally *de novo* designed[11] to bind PZn−Ph−NDI in an interior consisting of hydrophobic amino acids (Figure 4 and Supporting Information). Electronic absorption and circular dichroism spectra of the complex in aqueous buffer confirm 1:1 binding of PZn−Ph−NDI to the interior of a helical protein and verify histidine coordination of

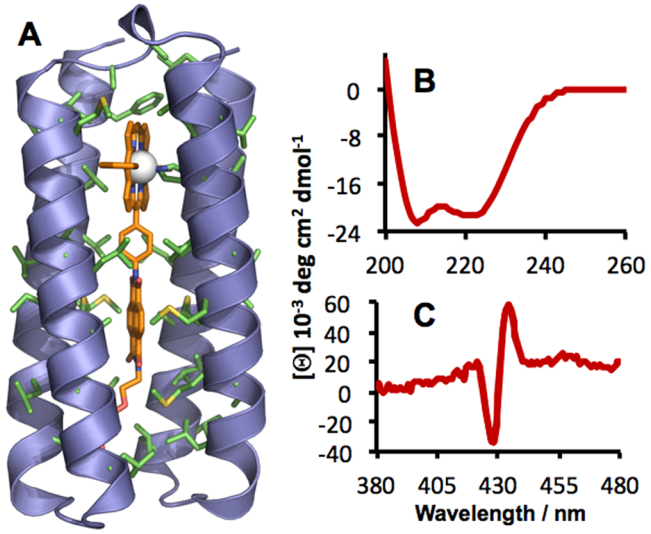

Figure 4. (A) Model of *SCPZnI3* showing interior hydrophobic residues (green) surrounding PZn−Ph−NDI (orange). (B,C) Circular dichroism spectra of *SCPZnI3* holoprotein. (B) Molar ellipticity per residue is consistent with a helical structure. (C) Molar ellipticity (Cotton effect) in visible region indicates that the achiral cofactor resides in a structured, chiral environment (see Figure S21).

DOI: 10.1021/jacs.5b13180
J. Am. Chem. Soc. 2016, 138, 2130−2133

the PZn moiety (Figure 4B,C, Figures S21−S23). Thus, the electronic environment of PZn−Ph−NDI is consistent with that of a protein interior.

The ET dynamics of PZn−Ph−NDI within the protein interior was monitored following electronic excitation of the PZn−Ph−NDI/*SCPZnI3* complex in D_2O buffer and analyzed via decay-associated difference spectra derived from global fitting of the multiwavelength transient data (Figure 5). The CR

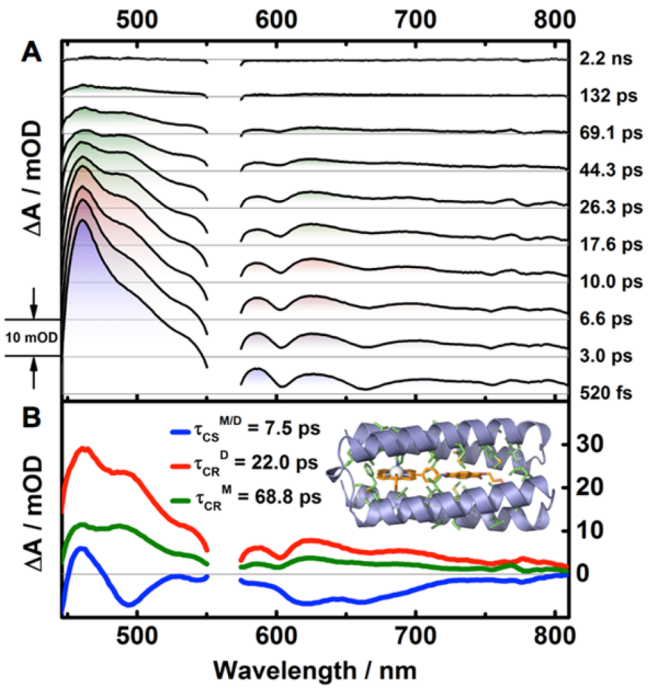

Figure 5. Pump−probe transient dynamics of PZn−Ph−NDI/*SCPZnI3* complex in D_2O buffer. (A) Transient dynamical data at pump−probe time delays labeled on the right. Each spectrum is offset by 10 mOD for clarity. (B) Decay-associated difference spectra (sans laser scatter at 560 ± 5 nm) with associated τ_{CR} and τ_{CS}. D and M superscripts refer to dimer and monomer, respectively. Experimental conditions: λ_{ex} = 560 nm, P_{ex} = 920 nJ/pulse, T = 21 °C, magic angle polarization.

dynamics of PZn−Ph−NDI in *SCPZnI3* are biexponential: we assign the dominant CR time τ_{CR} = 22 ps to the *SCPZnI3* holo-dimer, and the CR time τ_{CR} = 69 ps to the *SCPZnI3* holo-monomer, as their respective amplitudes track with the approximate 2:1 dimer/monomer ratio determined from analytical gel filtration (Supporting Information). CS occurs in monomer and dimer with the same time constant τ_{CS} = 7.5 ps. The overlapping distributions of τ_{CS} for *SCPZnI3*/H(D)$_2$O buffer (Figure 3) do not exhibit a KIE, indicating the lack of a significant role played by water in the CS event. On the basis of this observation, we conclude that PZn−Ph−NDI is sequestered from solvent within a well-packed protein interior in both the dimer and monomer.

By comparison with Figure 2, each ET time constant exhibited by PZn−Ph−NDI can be mapped to an effective ε_s. In the *SCPZnI3* holo-monomer, CS and CR time constants (τ_{CS} = 7.5 ps, τ_{CR} = 69 ps) cannot be uniquely mapped to a single effective ε_s that jointly recovers both time constants. Two distinct ε_s values are needed (Figure 2, green). Accounting for the relative errors in the measured time constants (Supporting Information), as well as the nonmonotonic nature of the CS dependence on solvent dielectric, the range of the effective ε_s that describes CS (τ_{CS} = 7.5 ps) is 8.3−13.4. We take $\varepsilon_S^{(CS)}$ = 8.3 as a lower limit. The effective ε_s describing CR is well-defined: $\varepsilon_S^{(CR)}$ = 3.0 ± 0.1. Indeed, CS resembles that in 99:1 THF/NMI ($\varepsilon_s \approx 8$), whereas CR resembles that in 99:1 dimethoxy-methane/NMI ($\varepsilon_s \approx 3$). Importantly, these assignments do not depend on any underlying model: they result from mapping dynamical data acquired for the *SCPZnI3* holoprotein onto an extensive body of analogous data obtained for PZn−Ph−NDI in widely varying dielectric environments. While a protein interior is not a uniform dielectric material, these ε_S values reflect the effective dielectric probed by PZn−Ph−NDI buried in the *SCPZnI3* interior, both pre- and post-charge separation.

How can the protein achieve such changes in dielectric on these fast (<100 ps) ET time scales? These results suggest a rigidification of the protein side chains upon formation of the $^{+\bullet}$PZn−Ph−NDI$^{\bullet-}$ CS state. Interestingly, the reduction in ε_S *after* the ET event suggests little solvational contribution to the CS state from polar water, despite the protein's small size, and contrary to commonly accepted views.[16] The dielectric constant is a key parameter affecting CS and CR rates in biological proteins. A ε_S-switching mechanism may warrant a reexamination of the energetic and electronic parameters derived from measurements of biological ET rates. Dielectric switching may provide a means to independently manipulate forward and back ET rates in natural catalytic proteins and artificial photosynthetic devices. Indeed, the ET time scales of PZn−Ph−NDI are similar to that of the primary ET in photosynthesis;[12] a decrease in protein ε_S upon the primary CS event would further slow wasteful inverted-regime CR in the photosynthetic reaction center.

■ ASSOCIATED CONTENT

Supporting Information

The Supporting Information is available free of charge on the ACS Publications website at DOI: 10.1021/jacs.5b13180.

Details regarding chemical synthesis, protein design and characterization, additional pump−probe spectra and methods, KIE data, a table of ET lifetimes of PZn−Ph−NDI in various solvents, and parameters for theoretical modeling of dielectric dependence of ET lifetimes (PDF)

■ AUTHOR INFORMATION

Corresponding Authors

*saven@sas.upenn.edu

*michael.therien@duke.edu

Present Addresses

[#]Argonne National Laboratory, Center for Nanoscale Materials, 9700 South Cass Avenue, Argonne, Illinois 60439, United States.

[▽]IBM Thomas J. Watson Research Center, Yorktown Heights, New York 10598, United States.

Author Contributions

[⊥]These authors contributed equally to this work.

Notes

The authors declare no competing financial interest.

■ ACKNOWLEDGMENTS

This work was supported through grants from the National Institutes of Health (R01 GM-071628) and the National Science Foundation (CHE-1413333).

DOI: 10.1021/jacs.5b13180
J. Am. Chem. Soc. 2016, 138, 2130−2133

REFERENCES

(1) (a) Alexov, E. G.; Gunner, M. R. *Biochemistry* **1999**, *38*, 8253−8270. (b) Schutz, C. N.; Warshel, A. *Proteins: Struct., Funct., Genet.* **2001**, *44*, 400−417. (c) Isom, D. G.; Castañeda, C. A.; Cannon, B. R.; Velu, P. D.; García-Moreno E, B. *Proc. Natl. Acad. Sci. U. S. A.* **2010**, *107*, 16096−16100. (d) Kukic, P.; Farrell, D.; McIntosh, L. P.; García-Moreno E, B.; Jensen, K. S.; Toleikis, Z.; Teilum, K.; Nielsen, J. E. *J. Am. Chem. Soc.* **2013**, *135*, 16968−16976.

(2) (a) Marcus, R. A.; Sutin, N. *Biochim. Biophys. Acta, Rev. Bioenerg.* **1985**, *811*, 265−322. (b) Steffen, M. A.; Lao, K.; Boxer, S. G. *Science* **1994**, *264*, 810−816.

(3) (a) Hammes-Schiffer, S.; Stuchebrukhov, A. A. *Chem. Rev.* **2010**, *110*, 6939−6960. (b) Glover, S. D.; Jorge, C.; Liang, L.; Valentine, K. G.; Hammarström, L.; Tommos, C. *J. Am. Chem. Soc.* **2014**, *136*, 14039−14051. (c) Migliore, A.; Polizzi, N. F.; Therien, M. J.; Beratan, D. N. *Chem. Rev.* **2014**, *114*, 3381−3465.

(4) (a) Warshel, A.; Papazyan, A. *Curr. Opin. Struct. Biol.* **1998**, *8*, 211−217. (b) Gray, H. B.; Winkler, J. R. *Proc. Natl. Acad. Sci. U. S. A.* **2005**, *102*, 3534−3539. (c) Li, L.; Li, C.; Zhang, Z.; Alexov, E. *J. Chem. Theory Comput.* **2013**, *9*, 2126−2136.

(5) Redmore, N. P.; Rubtsov, I. V.; Therien, M. J. *J. Am. Chem. Soc.* **2003**, *125*, 8769−8778.

(6) Gosztola, D.; Niemczyk, M. P.; Svec, W.; Lukas, A. S.; Wasielewski, M. R. *J. Phys. Chem. A* **2000**, *104*, 6545−6551.

(7) Hopfield, J. J. In *Protein Structure: Molecular and Electronic Reactivity*; Austin, R., Buhks, E., Chance, B., Dutton, P., De Vault, D., Frauenfelder, H., Gol'danskii, V., Eds.; Springer: New York, 1987; pp 167−185.

(8) (a) Kahlow, M. A.; Kang, T. J.; Barbara, P. F. *J. Phys. Chem.* **1987**, *91*, 6452−6455. (b) Maroncelli, M.; MacInnis, J.; Fleming, G. R. *Science* **1989**, *243*, 1674−1681.

(9) Kadish, K. M.; Shiue, L. R.; Rhodes, R. K.; Bottomley, L. A. *Inorg. Chem.* **1981**, *20*, 1274−1277.

(10) (a) Buhks, E.; Bixon, M.; Jortner, J. *J. Phys. Chem.* **1981**, *85*, 3763−3766. (b) Shirota, H.; Pal, H.; Tominaga, K.; Yoshihara, K. *J. Phys. Chem. A* **1998**, *102*, 3089−3102.

(11) (a) Bender, G. M.; Lehmann, A.; Zou, H.; Cheng, H.; Fry, H. C.; Engel, D.; Therien, M. J.; Blasie, J. K.; Roder, H.; Saven, J. G.; DeGrado, W. F. *J. Am. Chem. Soc.* **2007**, *129*, 10732−10740. (b) Calhoun, J. R.; Kono, H.; Lahr, S.; Wang, W.; DeGrado, W. F.; Saven, J. G. *J. Mol. Biol.* **2003**, *334*, 1101−1115. (c) Cochran, F. V.; Wu, S. P.; Wang, W.; Nanda, V.; Saven, J. G.; Therien, M. J.; DeGrado, W. F. *J. Am. Chem. Soc.* **2005**, *127*, 1346−1347. (d) Fry, H. C.; Lehmann, A.; Saven, J. G.; DeGrado, W. F.; Therien, M. J. *J. Am. Chem. Soc.* **2010**, *132*, 3997−4005. (e) Fry, H. C.; Lehmann, A.; Sinks, L. E.; Asselberghs, I.; Tronin, A.; Krishnan, V.; Blasie, J. K.; Clays, K.; DeGrado, W. F.; Saven, J. G.; Therien, M. J. *J. Am. Chem. Soc.* **2013**, *135*, 13914−13926.

(12) (a) Carter, B.; Boxer, S. G.; Holten, D.; Kirmaier, C. *Biochemistry* **2009**, *48*, 2571−2573. (b) Heller, B. A.; Holten, D.; Kirmaier, C. *Science* **1995**, *269*, 940−945. (c) Wasielewski, M. R.; Johnson, D. G.; Seibert, M.; Govindjee. *Proc. Natl. Acad. Sci. U. S. A.* **1989**, *86*, 524−528.

DOI: 10.1021/jacs.5b13180
J. Am. Chem. Soc. 2016, 138, 2130−2133